Article

Highly Monodisperse, Size Tunable Glucosamine Conjugated CdSe Quantum Dots for Enhanced Cellular Uptake and Bioimaging

Shamili Bandaru, Mathangi Palanivel, Manaswini Ravipati, Wen-Ya Wu, Syed Zahid, Surfarazhussain S. Halkarni, Goutam Kumar Dalapati, Krishna Kanta Ghosh, Balázs Gulyás, Parasuraman Padmanabhan,* and Sabyasachi Chakrabortty*

Read Online

ACCESS | ᴵᴵ Metrics & More | 🖺 Article Recommendations | 🆂🅸 Supporting Information

ABSTRACT: Semiconductor quantum dots (QDs) have been used in a variety of applications ranging from optoelectronics to biodiagnostic fields, primarily due to their size dependent fluorescent nature. CdSe nanocrystals (NCs) are generally synthesized via a hot injection method in an organic solvent. However, such NCs are insoluble in water and therefore preclude the direct usage toward biological systems. Thus, the preparation of more biocompatible water-soluble QDs with a high photo-luminescent quantum yield (PLQY) is extremely important for imaging applications. Although previous literature has detailed on the synthesis of CdSe NCs in water, they suffer from poor size distribution and very low PLQY. The complex formation mechanism of CdSe NCs in an aqueous environment adversely affects the quality of NCs due to the presence of OH⁻, H+, and H_2O moieties. Here in this article, we have presented the facile hydrothermal approach to obtain size tunable (2.9−5.1 nm), aqueous CdSe NCs with a narrow emission profile having ~40 nm fwhm with 56% PLQY. Physicochemical properties of the synthesized water-soluble CdSe NCs were studied with the help of UV− vis, PL, XRD, FTIR, XPS, and HR-TEM analysis. Furthermore, the surface of the synthesized CdSe NCs was modified with D-glucosamine via EDC and NHS coupling to obtain a stable, biocompatible bioimaging probe. Furthermore, we demonstrated that their successful bioconjugation with glucosamine could facilitate effective internalization into the cellular matrix.
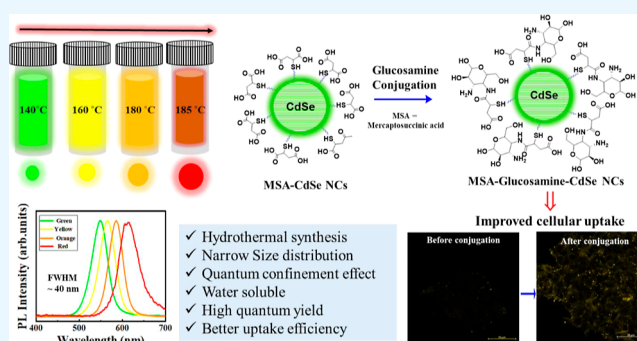
1. INTRODUCTION

In the field of nanomaterials, three dimensionally confined quantum dots (QDs) have drawn much attention because of their unique size-dependent optoelectronic properties.[1] Several compositions of metal chalcogenide such as ZnS, ZnSe, CdTe, CdS, and CdSe have been synthesized and widely used in solar cells, photovoltaic sensors, biological imaging and multimodal imaging, photocatalysis, and light emitting diodes.[2] Among the above-mentioned QDs, nanosized cadmium selenide (CdSe) semiconductor NCs are most studied and highly attractive with promising application in biomedicine.[3,4] Their photostability, broad absorption cross-section, and wide tunable emission profile across the entire visible region render CdSe NCs as a potential biolabeling candidate, as compared to conventional fluorescent dyes.[5,6] In general, high quality CdSe NCs have traditionally been synthesized in organic medium via a hot injection method using long chain hydrocarbons as ligands.[7] This method had been widely utilized due to the outcome of monodispersed, high yield NCs with negligible surface defect states. However, such CdSe NCs obtained in the organic phase are insoluble in water and therefore precludes the direct usage toward biological systems.[8] Therefore, the direct synthesis of

CdSe NCs in aqueous medium or successful hydrophilic ligand exchange to get water-soluble CdSe NCs have remained an attractive area of research, especially as bioimaging agent.

For instance, organometallic synthesis route in aqueous solvent, ligand exchange,[9,10] direct one pot synthesis at inert atmosphere, and post preparative treatment[11] were some of the techniques that have successfully yielded CdSe NCs in aqueous media. However, these NCs possess a lower quantum yield (QY) and very broad emission spectra that were preliminary due to the poor surface passivation and monodispersity issues. In general, the chemical reaction in the aqueous phase involves a complex mechanism due to the presence of OH⁻, H⁺, and H_2O moieties, which eventually protonate or deprotonate the ligands, resulting in the introduction of surface traps by which fluorescence is strongly
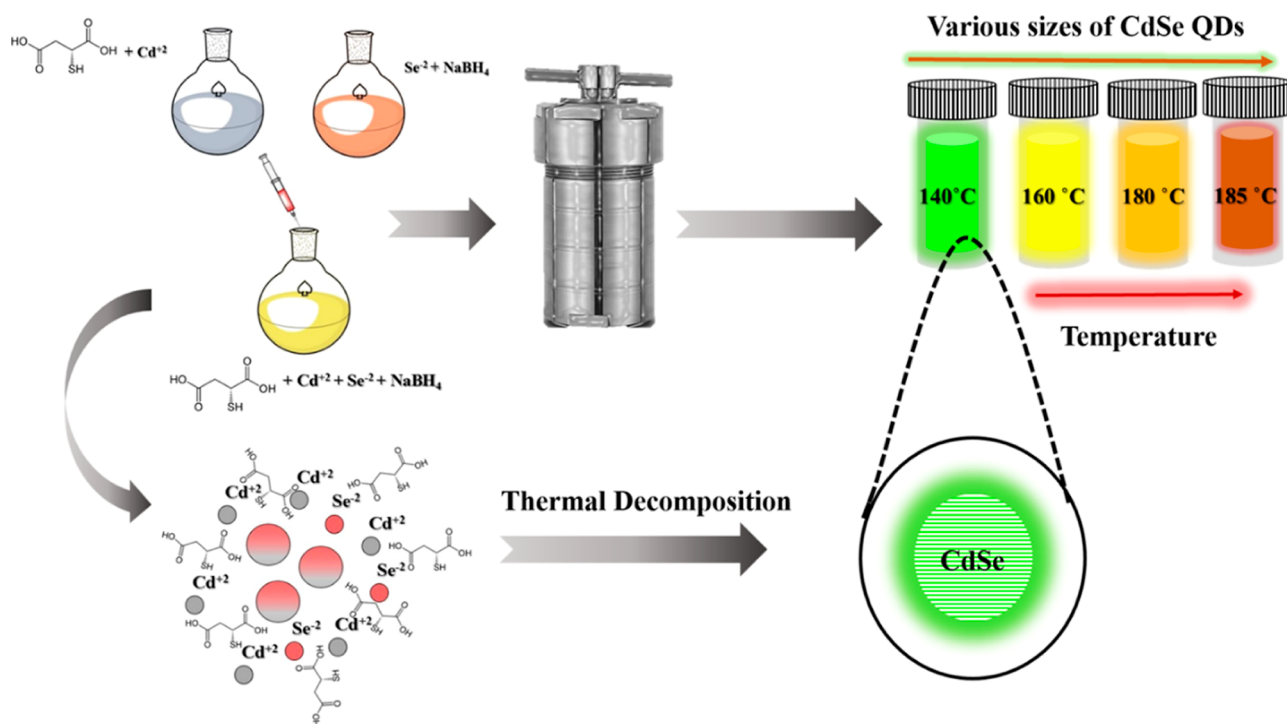
Figure 1. Schematic diagram of the procedure involved in the synthesis of size tunable CdSe NCs.

affected.[8] On the other hand, a low boiling point and complex ionic environment adversely affect the quality of NCs and hence result in a low emission QY and wide full width at half maxima (fwhm). Despite these limitations, hydrothermal methods could provide access to the synthesis of water-soluble high quality NCs at elevated temperatures with tunable morphologies by changing the temperature.[12] In this sense, the hydrothermal method turns out to be an excellent alternative when compared to others (i.e., microwave assisted method, heating method, etc.) with advantages of environmental amiable, low cost synthesis tool that is suitable for large scale production with controlled NCs growth.

Due to their small size, superior emission characteristics, ease of surface functionalization, and photostability properties, it is well-known that CdSe NCs are a potential tool for bio labeling. However, the cytotoxicity of CdSe due to the leaching of Cd ions from the NCs limits their usage in biological applications especially in the high concentration regime. To overcome this, a surface functionalization strategy could be beneficial, whereby modifying the surface with various biomolecules, for imparting the bioactivity and/or biocompatibility issues. In particular, simple chemical conjugation of NCs with biomolecules that improve cellular uptake is favorable for the usage of NCs in bio labeling and therapeutic applications.[13] It is well-known that cancerous cells consume large amount of glucose[14] when compared to normal cells. Thus, glyco-conjugation is one of the prominent strategy to targeting such kind of cancer cells.[15] We hypothesized that the conjugation with D-glucosamine, an earth abundant sugar, with CdSe NCs is expected to boost NCs cellular uptake.[16] Besides, bioconjugation also help to alleviate the toxicity caused by CdSe NCs. Amide-based conjugation is a well-known strategy in chemical functionalization to impart water solubility where capping agents play a crucial role in the chemical synthesis.[17] We chose thiol as chemical functionality by analyzing the hard soft acid base (HSAB) theory in Cd and

Se that showed strong interactions with the −SH group.[8] Thus, mercaptosuccinic acid (MSA) was chosen as a stabilizing agent to provide colloidal stability and interface for the conjugation of biomolecule. Apart from chemical leaching, photothermal property limits NCs in bioimaging application. Light induced elevation of surrounding temperature in cells may trigger various hazardous circumstances (i.e., denature of protein, evaporation of cytosol, and lysis of cell membrane by leading to cell death). Thus, fluorescent materials without the hyperthermia property were highly appreciated in bioimaging applications.[18]

Herein, we have synthesized high quality, monodisperse, size tunable, narrow emission profile, and water-soluble CdSe NCs via a facile hydrothermal method. Mainly, the alteration of temperature in the synthesis protocol played the vital role to obtain such NCs. The optical characteristics of the as-synthesized NCs were evaluated using UV−visible spectroscopy, photoluminescence (PL) spectra, and lifetime decay using time-resolved photoluminescence (TRPL). An emergence of a better crystalline phase was obtained using X-ray diffractometer (XRD). Furthermore, the surface passivation of MSA on the surface of NCs was analyzed with the help of Fourier transform infrared spectroscopy (FTIR) and surface chemical oxidation states using X-ray photoelectron spectroscopy (XPS). In addition, the tunable morphology, monodispersity, lattice spacing, and average sizes of the NCs at different temperatures were calculated through high resolution transmission electron microscopy (HRTEM). These NCs can serve as an excellent bioimaging agent as their photothermal evaluation suggested that they did not heat up during light irradiation. Furthermore, we aimed to show that a significant improvement in their uptake was observed with the conjugation of D-glucosamine biomolecule conjugation. Furthermore, we have performed D-glucosamine bio conjugation on the surface of CdSe NCs via an amide-linkage. Finally, the improved cellular uptake of various sized CdSe

NCs with glucosamine conjugation on human embryonic kidney (HEK) cell-lines was captured with a confocal microscope.

2. MATERIALS AND METHODS

2.1. Chemicals. Cadmium chloride monohydrate [$CdCl_2 \cdot H_2O$, 98%] and sodium selenite anhydrous [Na_2SeO_3, 98%] were purchased from SRL chemicals. MSA [$C_4H_8O_4S$, 97%] purchased from Sigma-Aldrich, sodium borohydrate [$NaBH_4$, 98.00−102.00%] from HIMEDIA, and sodium hydroxide pellets [NaOH, 97%] purchased from FINAR were used in the synthesis without further purification.

2.2. Synthesis of CdSe QDs. High quality MSA-CdSe NCs were synthesized via a hydrothermal method using a two-precursor route. Initially, 5 mL of the selenium precursor was prepared by mixing 0.1 g of $NaBH_4$ and 0.2 mmol Na_2SeO_3 in 5 mL of deionized water and vigorously stirring until it changed color to red. During this process, a small outlet was connected to the vial for releasing the resultant hydrogen pressure in the vial. The obtained selenium precursor was stored at 4 °C until further use. The cadmium precursor was prepared by adding 0.4 mmol of $CdCl_2 \cdot H_2O$ to 20 mL of 2.7 mmol of MSA under vigorous stirring, followed by adjusting pH using 1 (M) NaOH. Eventually, 1 mL of the as-prepared selenium precursor was added to the cadmium precursor and stirred for 2−3 min. Then, the resultant mixture was transferred to a 100 mL Teflon lined stainless steel autoclave and incubated at different temperatures (140, 160, 180, and 185 °C) for 45 min to acquire size tunable water-soluble semiconductor CdSe NCs. Finally, the obtained NCs were washed with ethanol and copious amounts of water and dispersed in deionized water for further use. The schematics of the synthesis process are shown in Figure 1.

2.3. Experimental Methodology for Glucosamine Conjugation to CdSe. Glucosamine conjugated CdSe NCs were prepared by adding 10 mg of CdSe NCs to the 400 μL of EDC-NHS solution containing 30−40 mg of EDC and NHS. Then the mixture was allowed to stir for 1 h at room temperature. After the EDC-NHS activation, 30 mg of glucosamine was added to the EDC-NHS activated CdSe mixture followed by stirring for 24 h at room temperature. Obtained glucosamine conjugated CdSe NCs were centrifuged several times for 15 min at 14,000 rpm and purified by discarding the supernatant without disturbing pellet. Final glucosamine−CdSe NCs were resuspended in 300−400 μL of deionized water stored at 4 °C for future use. The samples were stable for months, and in general, they were used for the biological cell labeling experiments within 1 week of synthesis.

2.4. Instrument Details. *2.4.1. UV−visible Spectroscopy.* Measurements of absorbance and PL were performed under XENON lamp illumination using the Spark M model microplate reader. The Greiner-96 well plate (200 μL volume) was used for both absorbance (transparent) and fluorescence intensity scan (black well plate). 100 μL portion of each sample was loaded for the measurement.

2.4.2. Fourier Transform Infrared Spectroscopy. FTIR measurements were carried out using the ALPHA-II's attenuated total reflectance (ATR) mode by Bruker Optik GmbH. Globar IR sources (silicon carbide detectors) were used to generate the electromagnetic spectrum. A simple drop-casting technique was used to prepare thin films on the glass substrates. About 150 μL of each sample was drop-casted on 1.5 × 1.5 cm glass slide. IR spectroscopy between 4000 and

400 cm^{-1} was recorded. Later on, the OPUS/IR software was used to analyze the spectral data.

2.4.3. Transmission Electron Microscopy. A JEOL-JEM 2100 high resolution transmission electron microscope was used to capture bright field TEM images at a voltage of 200 kV. 5−10 μL of diluted sample was drop-casted on the copper grid (200 mesh, from TED PELLA) and allowed to dry overnight at room temperature. Obtained TEM images were further analyzed using ImageJ software.

2.4.4. Time Resolved Photoluminescence. TRPL measurements were carried out by using a time-correlated single photon counting (TCSPC - Horiba Jobin Yvon IBH) spectrometer. The laser diode (Delta Diode 425L) with a peak power 230 mW and the standard optical pulse-width ∼100 ps can be generated at repetition rates up to 100 MHz. An excitation laser source with a peak wavelength of 425 nm is used to measure the sample lifetime, which is a range of 200 ns. Further analysis of the PL decay curves was performed using IBH DAS6 software.

2.4.5. X-ray Photon Spectroscopy. The chemical states of the sample were determined by using XPS measurements which was equipped with Mg Kα (1253.6 eV) radiation (PHI VersaProbe III), with a detection angle of 45 °C, using pass energies at the analyzer for survey spectra as 55 eV and detailed spectra as 280 eV, respectively. The exact surface spot size of the sample (5 × 5 μm) was selected for the XPS analysis. To compensate for the charge effects of the surface, electrons from a flood gun (20 A) were used to neutralize the samples. Binding energies (B.E) of Cd, Se, and O in CdSe sample were recorded with a resolution of 0.5 eV after the surface sputtering.

2.4.6. Zeta Potential. The zeta potential measurements were carried out in a double-layered electrical cell, at 25 °C, using a Malvern Zetasizer Nano ZS. About 500−600 μL of diluted sample was used for the measurement.

2.5. Cell Culture for Uptake of CdSe NCs by HEK293T cells. The cellular uptake of size series tunable CdSe NCs was investigated with HEK293T cells, as described below. Cells of passage number 20 were seeded on ethanol-soaked and sterilized coverslips at a density of 150,000 cells per well in a 12-well plate. They were maintained in standard 1× DMEM (Gibco, NY, USA), 10% fetal bovine serum (Gibco, NY, USA), and 1% penicillin−streptomycin (Gibco, NY, USA) for 24 h until the cells reached 70 to 80% confluency. On the next day, old media was aspirated, and the cells were washed once with 1× PBS (Gibco, NY, USA). Following that, the various NCs (green, yellow, orange emitting NCs) diluted to a final concentration of 10 μg/mL in 1× DMEM (containing 1% penicillin−streptomycin) were added to the respective wells. The cells were incubated with the NCs at 37 °C for 4 h. Following incubation, the media was removed, and cells were washed thrice with 1× PBS. Thereafter, the cells were fixed in 3.7% paraformaldehyde (diluted in 1× PBS) for 15 min at 37 °C. The cells were then washed thrice with 1× PBS. The coverslips were mounted with ProLong gold antifade mountant (ThermoFisher, MA, USA) and stored at −20C until imaging. In addition, to study the enhancement in cellular uptake and decrease in cell toxicity with the biomolecule conjugation, cells were treated for 4 h with Glu-CdSe and bare CdSe NCs at high concentrations of 250 and 500 μg/mL. All fixed slides were imaged with the Zeiss laser scanning microscope (LSM) 800 (Zeiss, Oberkochen, Germany) at 63× oil magnification. The NCs were acquired using the 561
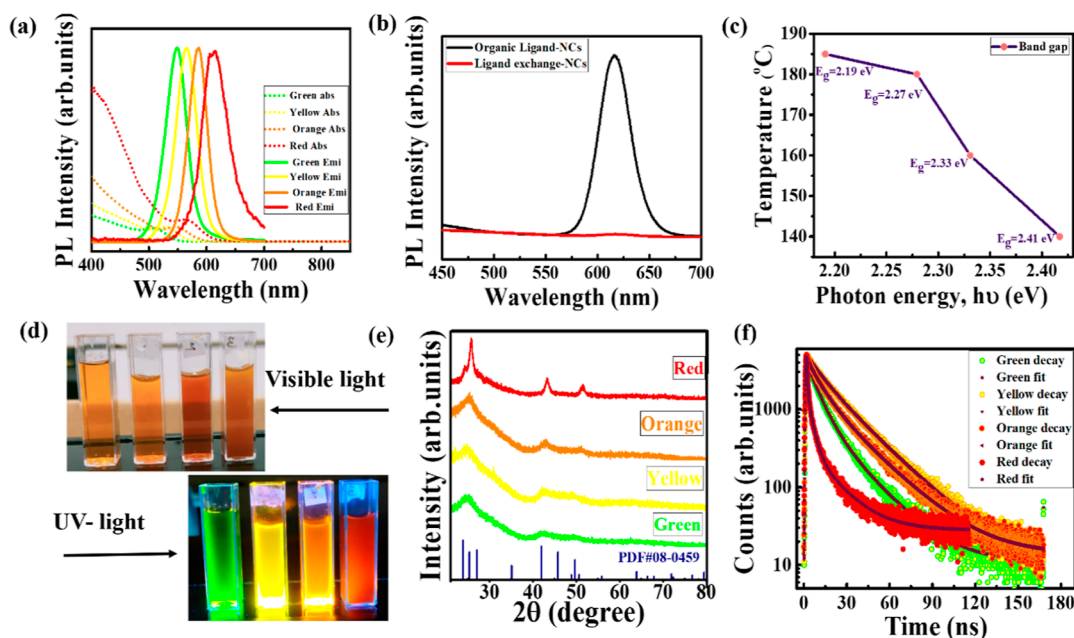
Figure 2. (a) UV−vis and PL spectra of as-synthesized size series tunable CdSe NCs; dotted line represents UV−vis spectra and solid line represents PL spectra, (b) change in optical properties (PL) of NCs synthesized in organic medium before (black line) and after (red line) the ligand exchange process, (c) "tauc plot" plotted to understand the band gap tunability upon temperature variation in their synthesis, (d) digital image under visible and hand-held UV lamp showed the PL behavior of each CdSe NCs, (e) XRD pattern of size series CdSe NCs which matched with the standard JCPDS card, (f) PL lifetime decay of all 4 size series NCs.

Table 1. Recent Literature on the Synthesis of Water-Soluble CdSe NCs Involving Various Parameters

s. no.	QDs	source used in synthesis	reaction condition	temperature	time	tunability (emission)	fwhm	PLQY	references
1	MSA-CdSe	water bath	ambient atmosphere	30	60 min	not stated	150 nm	29.7%	20
2	TGA and TSC-CdSe	magnetic stirring	ambient atmosphere	90	0−4 h	420−725 nm	not stated but broad peak observed	not stated	21
3	NAC-CdSe	magnetic stirring	N$_2$ atmosphere for 2 h	100	45 min	554 nm	not stated but broad peak observed	11.03%	22
4	NAC-CdSe	hydrothermal	N$_2$ atmosphere	200	70 min	540−555 nm	32 nm	25%	23
5	MSA-CdSe	hydrothermal	ambient atmosphere	140−185	45 min	545−616	40 nm	56%	this work

laser line (laser intensity: 2.00%; scan mode: frame; scan zoom: X and Y = 0.5; scan direction: unidirectional; averaging).

3. RESULTS AND DISCUSSION

Narrow emission, tunable CdSe NCs were synthesized in aqueous medium using a one-step hydrothermal process. The change in physicochemical properties, (optical properties, crystalline structure, and morphology) of as-synthesized CdSe NCs at various synthesis conditions (temperature alteration) were characterized using UV−vis Spectroscopy, PL, XRD, and HR-TEM. Figure 2a depicts the UV−vis and PL spectra of synthesized size series CdSe NCs, where the dotted lines indicate the absorbance, and the solid lines indicate PL spectra. The UV−vis spectra show that the tunable first excitonic absorbance peak of CdSe NCs ranges from 513 to 566 nm. Simple variation of the synthesis temperature from 140−185 °C led to the formation of size tunable CdSe NCs. Interestingly, these NCs possessed narrow size distribution as evaluated from the observed fwhm analysis. Especially, this distribution may open up their usefulness in using them as novel bioimaging agent in many advantages; (a) the direct use

of aqueous phase synthesized NCs for in vitro studies, (b) less overlap in their emission wavelength while using multiplexing application, and (c) we can obviate the use of hydrophilic ligands to perform surface functionalization for better availability in biological environment. In general, NCs synthesized in the organic medium have sharp emission properties with a better QY. However, as mentioned earlier, because of their hydrophobic long chains, and water-insoluble ligands, they were unable to be used in biological applications.[8] Later, the use of hydrophobic ligands to exchange the NCs surface was routinely done as a strategy to make them water-soluble. However, these processes introduced many trap states (due to surface state alteration)[9,19] and low colloidal stability of NCs. As a result, the NCs experienced severe quenching of their fluorescence emission and may not be useful for bioimaging experiments. Figure 2b shows one such case, where we have performed with a hydrophilic ligand, i.e., MSA exchange with organic ligand capped CdSe NCs under ambient condition. A sharp decrease in their emission characteristic proved that development water-soluble, stable, narrow emission profile NCs were crucial for better bioapplications.

Green emitting CdSe NCs synthesized at 140 °C show a sharp narrow emission at 545 nm when excited at 365 nm.

Table 2. Lifetime Decay Results and Analysis of Tunable Size Series NCs with Tri-Exponential Functional Parameters and Surface Charge Zeta Potential Values

s. no.	synthesis condition (°C)	emission	decay profile							zeta (mV)	size (nm)	fwhm (nm)
			avg decay(ns)	fitting parameters								
				$t1$	$a1$	$t2$	$a2$	$t3$	$a3$			
1	140	green	13	7.60×10^{-9}	48.99	8.53×10^{-10}	7.06	2.16×10^{-8}	43.95	−14.9	2.9	40
2	160	yellow	21	9.60×10^{-0}	17.37	2.41×10^{-8}	81.62	6.69×10^{-10}	1	−36.6	3.1	41
3	180	orange	18	9.11×10^{-9}	33.61	2.45×10^{-8}	62.84	1.39×10^{-9}	3.55	−33.6	4	41
4	185	red	6.8	3.47×10^{-9}	33.53	1.76×10^{-8}	31.22	4.59×10^{-10}	35.24	−29.1	5.1	54
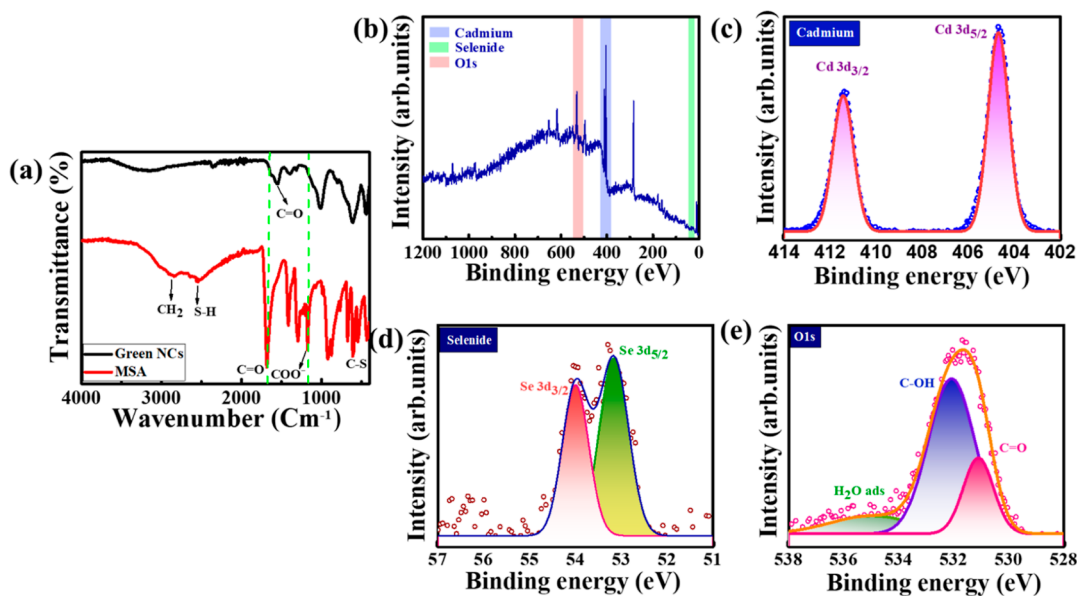
Figure 3. Surface analysis of green CdSe NCs (a) FT-IR spectra of bare MSA (red line) and MSA-CdSe NCs (black line), (b) XPS spectra of low resolution survey scan of CdSe NCs, (c) high resolution scan of Cd element which exhibits two sharp characteristic binding energy peaks for the presence of Cd $3d_{5/2}$ and Cd 3d $_{3/2}$ electronic states, (d) high resolution scan of Se element with characteristic binding energy peaks for $3d_{5/3}$ and Se $3d_{3/2}$ electronic state, (e) high resolution spectra of the O 1s binding energy peak attributed to the chemisorption oxygen.

Thus, the observed Stokes shift between the excitonic and emission spectra is nearly 32 nm, implying the PL emergence from the excitonic emission. Furthermore, with the subtle increase in synthesis temperature from 140 to 160, 180, and 185 °C, the emission profiles of the tunable size series CdSe NCs had symmetrically red-shifted from 545 to 565, 586, and 616 nm, respectively. Depending on the obtained excitonic spectra, the band gaps of the size series of CdSe NCs were calculated using a tauc relation equation. It was observed that band gap decreased from 2.41 to 2.19 eV with an increase in temperature from 140−185 °C, which is wider as compared to bulk CdSe (1.74 eV) due to the quantum confinement effect.[20] The band gap against temperature was plotted and is shown in Figure 2c. A redshift in PL and absorbance with a decrease in band gap clearly indicates the increase in size of NCs with increasing temperature, which will be substantiated later through TEM. The respective digital images of the tunable emission (green, yellow, orange, and red) under visible and UV light are shown in Figure 2d. The relative photoluminescence QY (PLQY) for the obtained CdSe NCs was calculated, and about 56% of PLQY was obtained for yellow emission NCs, which is higher than the previous reports (as shown Table 1). Taken together, we have synthesized CdSe NCs via a facile hydrothermal method in a very short time (∼45 min) that

showed a narrow emission profile, water solubility, and better QY as compared to others reported in literature (Table 1).

Furthermore, the crystalline structure of as-synthesized CdSe NCs was characterized by using XRD. Figure 2e reveals that the synthesized CdSe NCs exhibit three broad noisy diffraction peaks at 25.3 41.9, and 50.6° associated with the (002), (110), and (201) crystal planes due to its finite nondimensional crystal structure. The XRD pattern of the as-synthesized CdSe NCs is in good agreement with the standard CdSe card of the hexagonal wurtzite structure [PDF#08-0459]. However, the intensity of the 25.3° diffraction peak increased with increasing temperature, indicating the superior growth of crystal. Thus, the red emissive CdSe NCs showed better crystallinity with sharper XRD peaks. Additionally, to understand the carrier dynamics, radiative energy transfer processes, and interactions between electronic states, we have performed radiative lifetime decay[24] analysis of our synthesized NCs, which are shown in Figure 2f. In general, all of them were adapted to triexponential functional decay with average lifetime of 14, 21, 18, and 6.8 ns for green, yellow, orange, and red emission NCs, respectively. Direct recombination ($\tau 1$), defect state recombination ($\tau 2$), and deep traps recombination ($\tau 3$) contributed to observe the average lifetime of the samples where a1, a2, and a3 are their respective amplitudes.[25] $\tau 1$, $\tau 2$, and $\tau 3$ are the characteristic radiative
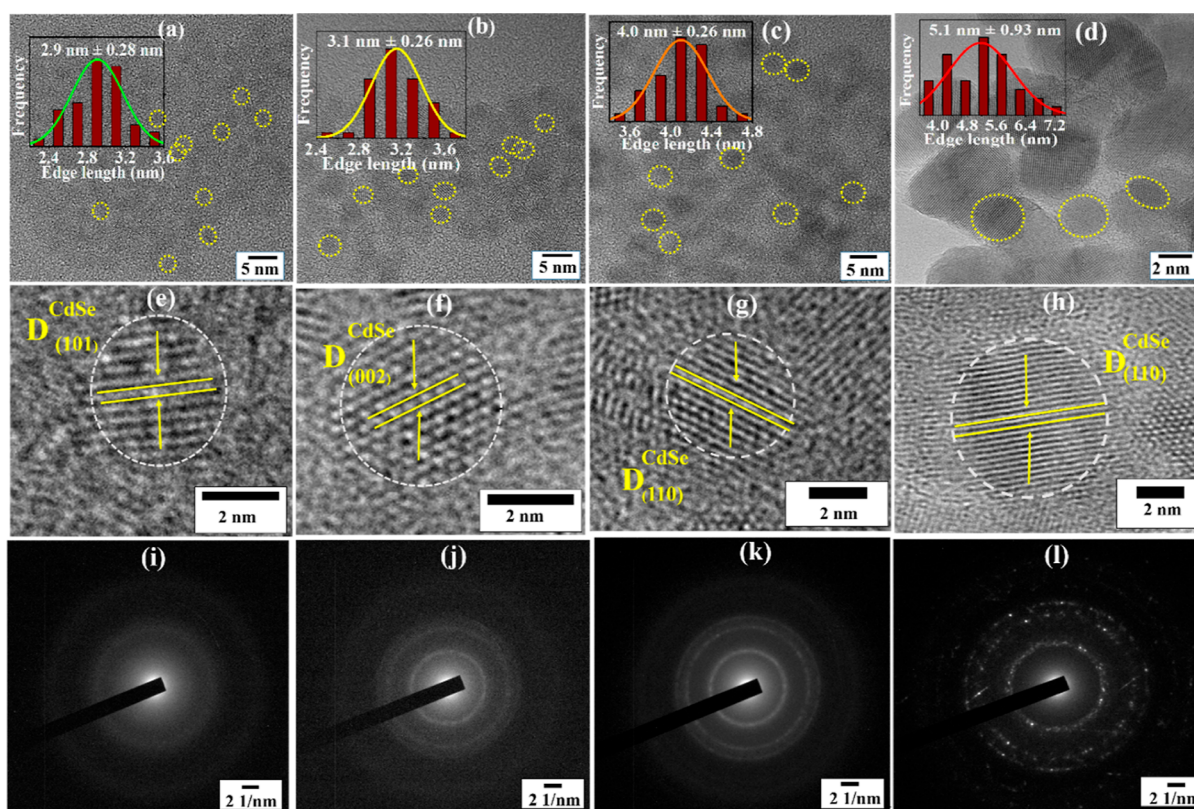
Figure 4. HR-TEM images of size tunable CdSe NCs; (a−d) High resolution images of the green, yellow, orange, and red NCs synthesized at different temperatures, and the inset represents the size distribution histogram; (e,h) crystal lattice spacing calculations of the respective NCs (i−l) represents the SAED pattern of NCs with improved crystallinity with increase in size and temperature.

decay times of different recombination for a three-exponential decay. The quantitative results and analysis for the NCs are tabulated and are shown in Table 2. However, no trend in lifetime decay was noted. We hypothesized that the relative increase in lifetime for NCs synthesized at 160 °C might be due to the formation of more ordered crystalline structures while comparing with NCs synthesized at 140 °C.[26] Furthermore, in response to an increase in reaction temperature to 185 °C, the average lifetime of NCs had decreased; plausibly due to the introduction of more nonradiative recombination in their surface. The observation of PLQY directly correlated with radiative decay pattern of these NCs. Therefore, we believe that this phenomena of increasing and decreasing PL decay is based on the thermodynamics of the crystalline structure[26] and the effect of stabilizing agents. Moreover, the colloidal stability of the synthesized tunable size series CdSe NCs was measured using the zeta potential. From Table 2, it was found that the zeta potential values of tunable size series NCs also follow a similar pattern. The net negative charge indicates the outward facing carboxylate anions related to MSA that provide colloidal stability through electrostatic and steric hindrance effects.[4,20]

The contribution of MSA functional groups in stabilizing the water-soluble CdSe NCs was analyzed using FTIR. FTIR spectra were recorded for both pure MSA and MSA-CdSe (green) for a better understanding of ligand passivation on the surfaces of NCs. From Figure 3a, it was observed that pure MSA exhibits sharp vibrational bands of carboxylic groups, encompassing stretching vibrations of C−O and C═O, and C−O−H bending vibrations at 1290.5, 1687.7, and 1411.9 cm^{-1} respectively. However, these bands of MSA undergo

changes when capped on the surface of CdSe and form symmetric and asymmetrical stretching vibrations of COO^{-} at 1543 and 1389 cm^{-1}, respectively in MSA-CdSe.[27] The broad peak at 3175.8 cm^{-1} indicates the O−H stretching bands of water molecules. In pure MSA, S−H stretching bands were observed at 2842.4 and 2562.5 cm^{-1}. On the other hand, a higher wavenumber shift of the S−H band was observed in MSA-CdSe alongside the disappearance of the band at 2842.4 cm^{-1}. We believe this was due to emergence of a new Cd−S bond among MSA sulfur and Cd site.[28] Thus, the capping of MSA on the surface of CdSe was confirmed through FTIR spectra.

Furthermore, the chemical states and compositions of the NCs were studied by using XPS. Figure 3b shows the low-resolution survey spectra of Cd, Se, and O elements and their presence. Figure 3c shows the high resolution peaks of the Cd 3d element, in which Cd exhibits two sharp characteristic binding energy peaks at 404.6 eV and 411.4 that can be attributed to the presence of Cd 3d$_{5/2}$ and Cd 3d$_{3/2}$ electronic states.[29] In the case of Se, the observed peaks were further deconvoluted into two contributions, as shown in Figure 3d. Deconvoluted binding energies at 53.1 and 54 eV correspond to the oxidation states of Se in 3d$_{5/3}$ and Se 3d$_{3/2}$ states.[30] The signals of O 1s were observed due to the existence of MSA on the surface of CdSe nanocrystals. In Figure 3e, a high-resolution spectrum of the O 1s binding energy peak was deconvoluted into three surface state contributions. Binding energies at 532.0 and 531.0 eV resemble the presence of C−OH, C═O electronic states, respectively, while the low intensity binding energy characteristic peak at 535.1 eV can be attributed to the chemisorption oxygen from the surface
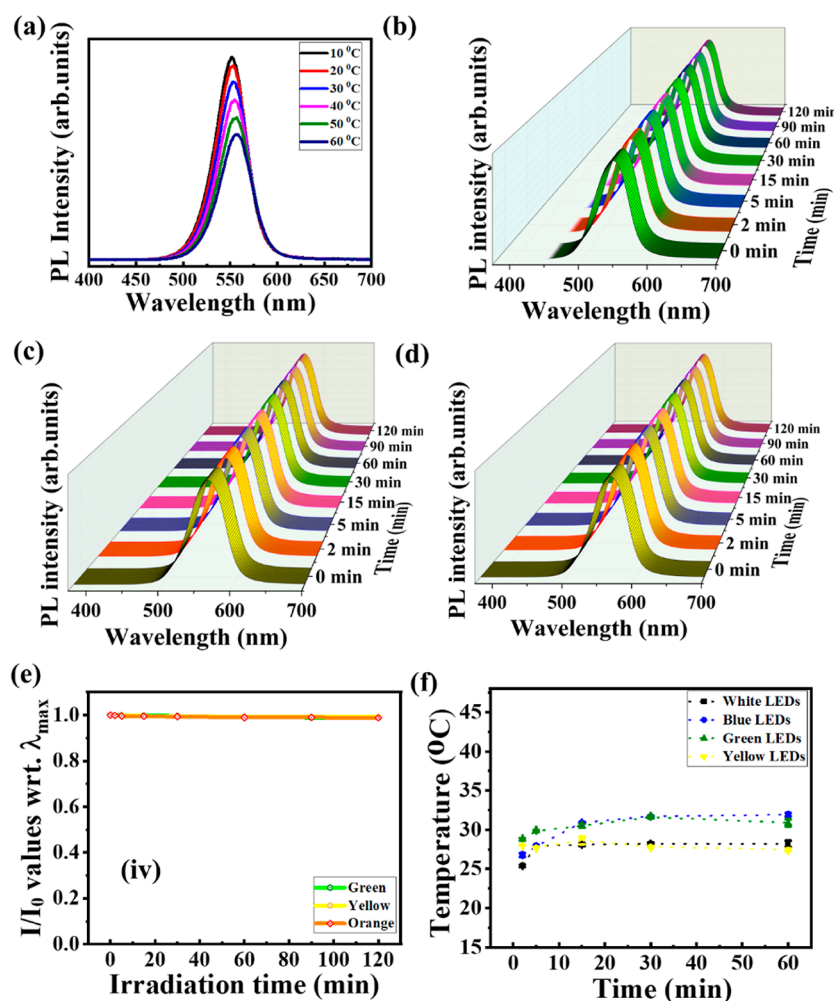
Figure 5. (a) Thermal stability of green emitting CdSe NCs recorded for every 10 °C linear increase up to 60 °C, (b−d) photostability of the NCs irradiated under blue LEDs which was recorded frequently for continuous irradiation until 120 min, (e) I/Io plot for the respective data shown on (b−d) and no decrease in the PL intensities were observed, and (f) photothermal property of green emitting CdSe NCs under blue, green, yellow, and white LED lights. Largely, they did not show any photothermal properties.

water.[21] Therefore, the XPS data confirm the surface states of Cd^{2+} and Se^{2-} elements in CdSe NCs.

HR-TEM analysis was performed to obtain insights into the morphological changes of CdSe NCs with respect to their variations in synthesis conditions (i.e., temperatures). Low resolution TEM images of green, yellow, orange, and red emitting CdSe NCs are demonstrated in Figure 4a−d, and corresponding high resolution TEM images are shown in Figure 4e−h. From the HR-TEM, it was observed that spherical and monodisperse nature of individual CdSe NCs were obtained at even synthesis temperatures up to 180 °C. While increasing the temperature further, it resulted in the formation of polydisperse NCs with irregular shapes. We believe further increasing in reaction temperature may not be kinetically and thermodynamically favorable to achieve monodisperse yet larger sized NCs. Approximately 50 particles were measured to obtain the average size of each NCs, and their respective graphical representation of the size distribution histogram is shown in the inset of Figure 4a−d. The histogram distribution curve demonstrates that the average size of NCs gradually increased from 2.9 to 5.1 nm (with a standard deviation of 0.2 nm) with increasing synthesis temperatures from 140 to 185C. This increase is in accordance with the

quantum confinement effect observed in their optical characteristics. The highest standard deviation (of 0.9 nm) was observed for NCs synthesized at 185C, denoting the incompetency of MSA as a successful surface passivator. Lattice spacings for the corresponding CdSe NCs were also calculated, and the obtained results were in good agreement with the XRD pattern. The existence of various crystalline lattice domains such as (101), (002), and (110) were observed in different CdSe NCs. From the selected area electron diffraction (SAED) pattern, a clear view of the increase in crystalline nature from 140 to 185 °C was observed, as shown in Figure 4i−l.

To understand the usefulness of these as-synthesized CdSe NCs in bioimaging applications, we have performed their thermal and photo stability tests under various conditions (Figure 5). The thermal stabilities of green, yellow, and orange emission CdSe NCs were recorded from 10 to 60 °C where a linear increase of 10 to 60 °C (Figures 5a and S2a,b) was observed. With increasing temperature, PL intensity of NCs decreased in all three-size series of NCs. These changes were attributed to the ligand passivation dynamics on the surfaces of CdSe NCs where a higher temperature might introduce more labile nature of the ligands.[31] Since our CdSe NCs had
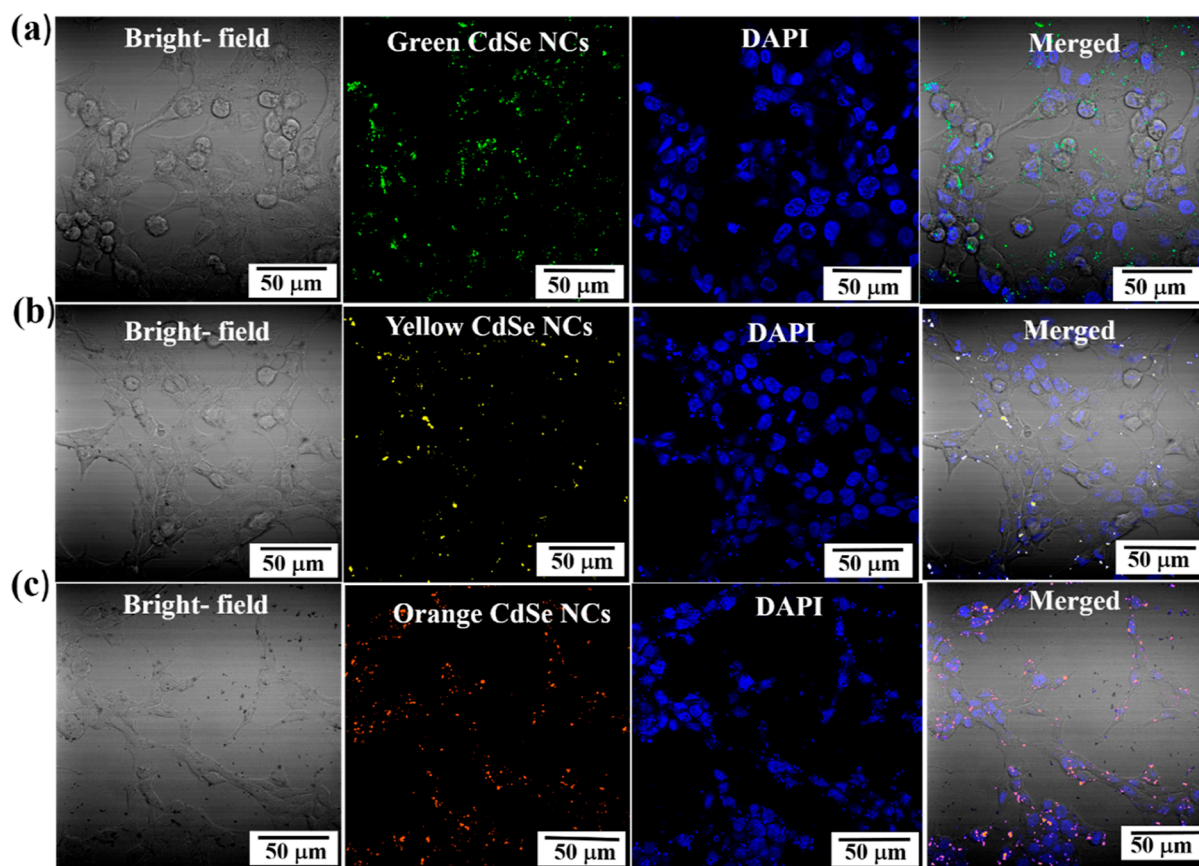
Figure 6. Bright-field, fluorescent, and merged confocal images of the uptake of (a) green, (b) yellow, and (c) orange emitting CdSe NCs by HEK293T cells that were captured after 4 h of incubation.

absorbance in the UV and visible regions, in addition to thermal stability, photosensitivity (i.e., photostability) tests of these size tunable CdSe NCs were also performed under continuous illuminations of commercially available light emitting diodes (LEDs) of different wavelengths. Green (Figure 5b), yellow (Figure 5c), and orange (Figure 5d) emitting NCs were irradiated under a blue LED (λ_{max}-470 nm) for 120 min, respectively. In addition, they were exposed to green LEDs (λ_{max}-529 nm) and white LEDs for the same time and the respective fluorescence spectra was recorded (Figure S3a,b). PL quenching was calculated under blue LED irradiation, and a very negligible quenching of 1.12 and 1.19% was experienced by green and orange emitting NCs, whereas yellow emitting NCs experienced only 0.8% quenching even after 120 min of continuous irradiation. The resultant I/I_0 (I is the initial intensity and I_0 is the change in intensity with respect to time) values for all three-size series NCs under blue LEDs were plotted against time and depicted in Figure 5e. Thus, negligible quenching of PL under blue, green, and white LEDs demonstrated excellent photostability of CdSe NCs. Furthermore, to comprehend the photothermal properties, temperature variation measurements under continuous light irradiation were performed with the help of a thermal camera. Briefly, 200 μL of each sample was irradiated under different LED irradiation, and the change in local temperature in the medium was recorded at different time intervals. The data obtained from the contour plot was shown in Figure 5f, and it was found that a very negligible change in temperature was observed under different LEDs for the green emitting CdSe NCs. The photothermal properties of yellow

and orange emitting CdSe NCs are shown in Figure S4a,b. Therefore, a clear indication of no substantial change in the rise of temperature in aqueous medium when the NCs were irradiated under different wavelength LEDs was demonstrated in the absence of photothermal property in our synthesized CdSe NCs. Thus, they would not affect the biological surroundings while being used as a diagnostic agent.

3.1. Cellular Uptake Study. Generally bioimaging is a noninvasive process used to record and visualize the 3D structure of a target in a specimen. However, the stability of the fluorescent material, physical interaction between NCs and cell membrane, and surface functionalization of NCs surface limit the bioimaging technique. In short, the major principle of the cell membrane is to oblige and protect the cells from exchange of external matter. Fluorescent nanomaterials which readily cross cell membranes are potential candidates for biological applications because of their aptness for the ability to internalize into cells. Thus, we have recorded both fluorescent and bright field images of the HEK293T cell line after incubated with green, yellow, and orange NCs without EDC-NHS activation and conjugation step, and results are illustrated in Figure 6a–c. Due to the strong fluorescence of green, yellow, and orange emitting NCs, it was easy to distinguish between the NCs and other subcellular organelles. Mainly the NCs were distributed in cytoplasm. The fluorescent punctate staining pattern in Figure 6a–c, whereby cells were incubated with NCs of all three-size series, confirmed the uptake of CdSe NCs of sizes 2.9, 3.2, and 4 nm for the green, yellow, and orange NCs, respectively. In the case of green NCs, some of the cells transform to a spherical-like shape after 24 h of

incubation, presumably due to elevated cell death caused by the smaller size and increased uptake of green NCs by the cells. However, in the other two cases, all of the cells survived well for more than a day. Time lapse videos of cellular uptake of the CdSe NCs over 24 h are depicted in Videos S7a, S7b, and S7c for different concentrations of NCs. It is also widely understood that bare or unstable CdSe NCs display greater levels of toxicity as compared to the core/shell structure or biomolecule encapsulated CdSe NCs due to the leaching of Cd ions from CdSe NCs, reducing the biocompatibility of such NCs in biological systems.

As mentioned before, the conjugation of a biomolecule to the CdSe NCs is required to reduce the toxicity to cells. In that respect, glucosamine conjugation might be an excellent choice because (a) glucose source for cancerous cells, (b) ease of functionalization through amide linkages, (c) pH of D-glucosamine (3.5−4.5) by which it supports the proton hypothesis in cells, and (d) hydrophilic nature makes NCs soluble in water. Thus, here in this work, we conjugated D-glucosamine to the surface of CdSe to attain stability, water solubility together with reduced toxicity (Glu-green NCs) (Figure S5). In general, the biomolecule functionalized CdSe improved the cell viability, where the effect was prominent in HEK293T cell lines as compared to Hela cell lines. Glucosamine conjugation on the surface of CdSe NCs was analyzed with FTIR and HRTEM (Figure S1a,b) and change in zeta potential value from −14 to +3.2 mV confirms the successful conjugation of glucosamine on the surface of CdSe. Stability of obtained Glu-green NCs was studied at different pHs (Figure S1c). Further, we have studied the cellular uptake of Glu-green NCs at high concentrations such as 250 and 500 μg/mL. From Figure 7a,b, it was observed that, when compared to bare MSA-green NCs, there was a huge increase in their cellular uptake characteristics of CdSe when treated with Glu-green NCs. Figure 7c represents the difference in corrected mean fluorescence between the biomolecule conjugated CdSe and MSA capped CdSe. Here, the cellular uptake was expected to increase because of CdSe surface functionalized with glucosamine, a biomolecule that enables the attachment of cell membrane due to its positive charge. Also generally, pH of D-glucosamine is acidic (3.5−4.5), by which it supports the proton hypothesis in cells involving endosome and lysosome escape. The obtained cellular images merged with DAPI are shown in Figure S6 to ensure that both CdSe and Glu-CdSe were inside the cells. Hence, we hypothesized the above reasons for enhanced cellular uptake of Glu-CdSe as compared to MSA-CdSe. Thus, the conjugation of the D-glucosamine strategy with strong fluorescent nature of CdSe NCs could be a viable alternative bioimaging technique. Furthermore, these NCs can be useful in investigating the distribution and tracking of the bioactive material in subcellular organelles to facilitate the drug delivery.

4. CONCLUSIONS

In summary, facile, one-step hydrothermal synthetic techniques were demonstrated to obtain size tunable, high QY, water-soluble CdSe NCs. Interestingly, they possessed a very narrow emission profile (a sharp ∼40 nm fwhm) as compared to the existing water-soluble CdSe NCs reported in the literature. This method could be an excellent alternative to obtain a high QY of ∼56% compared with ligand exchanged CdSe NCs if prepared from the organic solution process. In addition, the change in the synthesis temperature as the only varying parameter in the hydrothermal process displayed a systematic outcome of their tunable size with monodisperse shapes. The absorbance and emission profiles of the obtained CdSe NCs were evaluated using UV−vis, PL, and TRPL studies. PXRD confirmed the hexagonal crystalline nature of the NCs. Furthermore, systematic increase in size and the existence of the respective chemical elements in CdSe NCs was analyzed through HRTEM and XPS. Moreover, photostability, thermal stability, and photothermal attributes of these NCs were assessed, and insignificant alteration of their properties suggested meticulous usefulness of those as diagnostic agents. Later on, we demonstrated a successful bioconjugation of the CdSe NCs with glucosamine, facilitating their effective internalization into the HEK293T cellular matrix. Thus, the phenomena of improved cellular uptake via surface modified glucosamine conjugation can be applied in several in vitro applications such as biolabeling, bioimaging, and biosensing applications. Furthermore, they would act as a tracking drug delivery vehicle and guide the operative process in the biomedical field especially in personalized medicine.

■ ASSOCIATED CONTENT

Ⓢ Supporting Information

The Supporting Information is available free of charge at https://pubs.acs.org/doi/10.1021/acsomega.3c04962.

> Characterization of glucosamine conjugated CdSe NCs, ligand exchange methodology, MTT assay methodology, QY calculations, temperature dependent stability of yellow and orange emitting NCs, photostability under green and white LEDs, photothermal stability of yellow and orange emitting NCs, cell viability study (MTT assay) on HEK293T cells and HeLa cells (PDF)
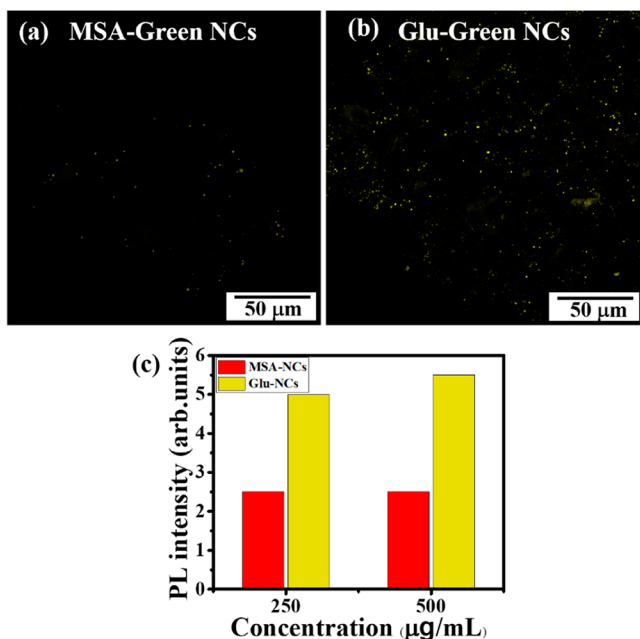
> Orange CdSe (MP4)

Figure 7. Cellular uptake of (a) MSA capped CdSe green NCs, (b) glucosamine conjugated CdSe green NCs, and (c) mean fluorescence difference between the CdSe with and without the conjugation of glucosamine molecule to the CdSe surface. Clearly, an improved uptake proved our hypothesis.

Yellow CdSe (MP4)

Green CdSe (MP4)

■ AUTHOR INFORMATION

Corresponding Authors

Parasuraman Padmanabhan − *Lee Kong Chian School of Medicine, Nanyang Technological University Singapore, Singapore 636921, Singapore; Cognitive Neuroimaging Centre, Nanyang Technological University, Singapore 636921, Singapore;* ○ orcid.org/0000-0003-4112-4600; Email: ppadmanabhan@ntu.edu.sg

Sabyasachi Chakrabortty − *Department of Chemistry, SRM University AP—Andhra Pradesh, Mangalagiri, Andhra Pradesh 522 240, India;* ○ orcid.org/0000-0002-2759-2208; Email: sabyasachi.c@srmap.edu.in

Authors

Shamili Bandaru − *Department of Chemistry, SRM University AP—Andhra Pradesh, Mangalagiri, Andhra Pradesh 522 240, India*

Mathangi Palanivel − *Lee Kong Chian School of Medicine, Nanyang Technological University Singapore, Singapore 636921, Singapore*

Manaswini Ravipati − *Department of Nanotechnology, Acharya Nagarjuna University, Guntur, Andhra Pradesh 522 240, India*

Wen-Ya Wu − *Institute of Materials Research and Engineering, Agency for Science, Technology and Research, Singapore 138634, Singapore;* ○ orcid.org/0000-0002-1557-1469

Syed Zahid − *Department of Mechanical Engineering, SRM University-AP, Mangalagiri, Andhra Pradesh 522 240, India*

Surfarazhussain S. Halkarni − *Department of Mechanical Engineering, SRM University-AP, Mangalagiri, Andhra Pradesh 522 240, India*

Goutam Kumar Dalapati − *Center for Nanofibers and Nanotechnology, Mechanical Engineering Department, National University of Singapore, Singapore 117576, Singapore*

Krishna Kanta Ghosh − *Lee Kong Chian School of Medicine, Nanyang Technological University Singapore, Singapore 636921, Singapore*

Balázs Gulyás − *Lee Kong Chian School of Medicine, Nanyang Technological University Singapore, Singapore 636921, Singapore; Cognitive Neuroimaging Centre, Nanyang Technological University, Singapore 636921, Singapore; Department of Clinical Neuroscience, Karolinska Institute, 17176 Stockholm, Sweden*

Complete contact information is available at:
https://pubs.acs.org/10.1021/acsomega.3c04962

Author Contributions

Conceptualization—S. B., P. P., S. C., and K. K.G.; methodology—S. B., M.R., M. P., and S. Z.; visualization—S. B., M. P., and S. Z.; validation—G. K. D., K. K. G., S. S.H., and S. C.; investigation—S. B., M. P., and S. C.; resources—W. W., S. S.H., P. P., B. G., S. C., and G. K.D.; data curation—S. B., S. C., and G. K.D.; writing—original draft—S. B., M. P., M.R., and S. C.; writing—review and editing—S. C., K. K.G., G. K.D., and W. W.; supervision—S.C., B. G., P. P., and K. K.G.; project administration—S. B., S.C., and G. K.D.; and funding acquisition—B. G., P. P., K. K. G., and S. C. All authors have read and agreed to the published version of the manuscript.

Notes

The authors declare no competing financial interest.

■ REFERENCES

(1) Dong, S.; Trivedi, D.; Chakrabortty, S.; Kobayashi, T.; Chan, Y.; Prezhdo, O. V.; Loh, Z.-H. Observation of an Excitonic Quantum Coherence in CdSe Nanocrystals. *Nano Lett.* **2015**, *15* (10), 6875−6882.

(2) Cotta, M. A. Quantum Dots and Their Applications: What Lies Ahead? *ACS Appl. Nano Mater.* **2020**, *3* (6), 4920−4924.

(3) Chan, W.; Shiao, N. Cytotoxic Effect of CdSe Quantum Dots on Mouse Embryonic Development. *Acta Pharmacol. Sin.* **2008**, *29* (2), 259−266.

(4) Zhang, M.; Bishop, B. P.; Thompson, N. L.; Hildahl, K.; Dang, B.; Mironchuk, O.; Chen, N.; Aoki, R.; Holmberg, V. C.; Nance, E. Quantum Dot Cellular Uptake and Toxicity in the Developing Brain: Implications for Use as Imaging Probes. *Nanoscale Adv.* **2019**, *1* (9), 3424−3442.

(5) Kim, S. H.; Man, M. T.; Lee, J. W.; Park, K.-D.; Lee, H. S. Influence of Size and Shape Anisotropy on Optical Properties of CdSe Quantum Dots. *Nanomaterials* **2020**, *10* (8), 1589.

(6) Xing, G.; Liao, Y.; Wu, X.; Chakrabortty, S.; Liu, X.; Yeow, E. K. L.; Chan, Y.; Sum, T. C. Ultralow-Threshold Two-Photon Pumped Amplified Spontaneous Emission and Lasing from Seeded CdSe/CdS Nanorod Heterostructures. *ACS Nano* **2012**, *6* (12), 10835−10844.

(7) Murray, C. B.; Norris, D. J.; Bawendi, M. G. Synthesis and Characterization of Nearly Monodisperse CdE (E = Sulfur, Selenium, Tellurium) Semiconductor Nanocrystallites. *J. Am. Chem. Soc.* **1993**, *115* (19), 8706−8715.

(8) Jing, L.; Kershaw, S. V.; Li, Y.; Huang, X.; Li, Y.; Rogach, A. L.; Gao, M. Aqueous Based Semiconductor Nanocrystals. *Chem. Rev.* **2016**, *116* (18), 10623−10730.

(9) Huang, Z.; Zeng, Q.; Bai, Z.; Qin, S. Regulating the Fluorescence Emission of CdSe Quantum Dots Based on the Surface Ligand Exchange with MAA. *Polym. Adv. Technol.* **2020**, *31* (11), 2667−2675.

(10) Wang, M.; Felorzabihi, N.; Guerin, G.; Haley, J. C.; Scholes, G. D.; Winnik, M. A. Water-Soluble CdSe Quantum Dots Passivated by a Multidentate Diblock Copolymer. *Macromolecules* **2007**, *40* (17), 6377−6384.

(11) Deng, B.-Y.; Wu, J.; Liu, J.; Ren, Y.-Y.; Wang, F. Facile Passivation of Yellow Light-Emitting CdSe QDs by Polyethyleneimine in Water to Achieve Bright White Light Emission. *Mater. Adv.* **2021**, *2* (22), 7384−7388.

(12) Gan, Y. X.; Jayatissa, A. H.; Yu, Z.; Chen, X.; Li, M. Hydrothermal Synthesis of Nanomaterials. *J. Nanomater.* **2020**, *2020*, 8917013.

(13) Wagner, A. M.; Knipe, J. M.; Orive, G.; Peppas, N. A. Quantum Dots in Biomedical Applications. *Acta Biomater.* **2019**, *94*, 44−63.

(14) Lin, X.; Xiao, Z.; Chen, T.; Liang, S. H.; Guo, H. Glucose Metabolism on Tumor Plasticity, Diagnosis, and Treatment. *Front. Oncol.* **2020**, *10*, 317.

(15) Calvaresi, E. C.; Hergenrother, P. J. Glucose Conjugation for the Specific Targeting and Treatment of Cancer. *Chem. Sci.* **2013**, *4* (6), 2319−2333.

(16) Igawa, K.; Xie, M.-F.; Ohba, H.; Yamada, S.; Hayashi, Y. D-Glucosamine Conjugation Accelerates the Labeling Efficiency of Quantum Dots in Osteoblastic Cells. *BioMed Res. Int.* **2014**, *2014*, 821607.

(17) Zrazhevskiy, P.; Sena, M.; Gao, X. Designing Multifunctional Quantum Dots for Bioimaging, Detection, and Drug Delivery. *Chem. Soc. Rev.* **2010**, *39* (11), 4326−4354.

(18) Eskiizmir, G.; Ermertcan, A. T.; Yapici, K. Nanomaterials: Promising Structures for the Management of Oral Cancer. In *Nanostructures for Oral Medicine*; Micro and Nano Technologies; Andronescu, E., Grumezescu, A. M., Eds.; Elsevier, 2017; Chapter 17, pp 511−544.

(19) Cao, Z.; Shu, Y.; Qin, H.; Su, B.; Peng, X. Quantum Dots with Highly Efficient, Stable, and Multicolor Electrochemiluminescence. *ACS Cent. Sci.* **2020**, *6* (7), 1129−1137.

(20) Viegas, I. M. A.; Santos, B. S.; Fontes, A.; Pereira, G. A. d. L.; Pereira, C. F. Multivariate Optimization of Optical Properties of CdSe Quantum Dots Obtained by a Facile One-Pot Aqueous Synthesis. *Inorg. Chem. Front.* **2019**, *6* (6), 1350−1360.

(21) Hashem, E. M.; Ahmed, M. A.; Abdel Messih, M. F. Facile One-Pot Aqueous Synthesis of Highly Soluble and Luminescent CdSe Quantum Dots without Nitrogen Bubbling. *CrystEngComm* **2020**, *22* (29), 4816−4822.

(22) Bala Subramaniyan, S.; Veerappan, A. Water Soluble Cadmium Selenide Quantum Dots for Ultrasensitive Detection of Organic, Inorganic and Elemental Mercury in Biological Fluids and Live Cells. *RSC Adv.* **2019**, *9* (39), 22274−22281.

(23) Wei, C.; Li, J.; Gao, F.; Guo, S.; Zhou, Y.; Zhao, D. One-Step Synthesis of High-Quality Water-Soluble CdSe Quantum Dots Capped by *N*-Acetyl-L-Cysteine *via* Hydrothermal Method and Their Characterization. *J. Spectrosc.* **2015**, *2015*, No. e369145.

(24) Singh, V.; Priyanka; More, P. V.; Hemmer, E.; Mishra, Y. K.; Khanna, P. K. Magic-Sized CdSe Nanoclusters: A Review on Synthesis, Properties and White Light Potential. *Mater. Adv.* **2021**, *2* (4), 1204−1228.

(25) Soni, U.; Pal, A.; Singh, S.; Mittal, M.; Yadav, S.; Elangovan, R.; Sapra, S. Simultaneous Type-I/Type-II Emission from CdSe/CdS/ZnSe Nano-Heterostructures. *ACS Nano* **2014**, *8* (1), 113−123.

(26) Rautaniemi, K.; Vuorimaa-Laukkanen, E.; Strachan, C. J.; Laaksonen, T. Crystallization Kinetics of an Amorphous Pharmaceutical Compound Using Fluorescence-Lifetime-Imaging Microscopy. *Mol. Pharmaceutics* **2018**, *15* (5), 1964−1971.

(27) Arivarasan, A.; Bharathi, S.; Ezhilarasi, S.; Arunpandiyan, S.; Jayavel, R. Photovoltaic Performances of Yb Doped CdTe QDs Sensitized TiO2 Photoanodes for Solar Cell Applications. *J. Inorg. Organomet. Polym.* **2019**, *29* (3), 859−868.

(28) Sanmartín-Matalobos, J.; Bermejo-Barrera, P.; Aboal-Somoza, M.; Fondo, M.; García-Deibe, A. M.; Corredoira-Vázquez, J.; Alves-Iglesias, Y. Semiconductor Quantum Dots as Target Analytes: Properties, Surface Chemistry and Detection. *Nanomaterials* **2022**, *12* (14), 2501.

(29) Subila, K. B.; Kishore Kumar, G.; Shivaprasad, S. M.; George Thomas, K. Luminescence Properties of CdSe Quantum Dots: Role of Crystal Structure and Surface Composition. *J. Phys. Chem. Lett.* **2013**, *4* (16), 2774−2779.

(30) Xiao, F.-X.; Miao, J.; Wang, H.-Y.; Yang, H.; Chen, J.; Liu, B. Electrochemical Construction of Hierarchically Ordered CdSe-Sensitized TiO2 Nanotube Arrays: Towards Versatile Photoelectrochemical Water Splitting and Photoredox Applications. *Nanoscale* **2014**, *6* (12), 6727−6737.

(31) Nawade, A.; Busi, K. B.; Ramya, K.; Dalapati, G. K.; Mukhopadhyay, S.; Chakrabortty, S. Improved Charge Transport across Bovine Serum Albumin−Au Nanoclusters' Hybrid Molecular Junction. *ACS Omega* **2022**, *7* (24), 20906−20913.